Coexpression of MTH1 and PMS2 Is Associated with Advanced Disease and Disease Progression after Therapy in Melanoma

JID Open

Journal of Investigative Dermatology (2021) ■, ■–■; doi:10.1016/j.jid.2021.07.166

TO THE EDITOR

Genomic instability is one of the hallmarks of cancer, and alterations in DNA damage response genes have been associated with sensitivity to immuno-oncology modulators (Mouw et al., 2017). Cutaneous malignant melanoma (CMM) is the cancer with the highest median tumor mutation burden (Alexandrov et al., 2013). Tumor mutation burden and DNA damage response have been demonstrated to have an impact on disease progression and therapy efficacy in CMM.

Immunotherapies with immune checkpoint inhibitors (ICIs), such as anti-PD1 and anti-CTLA4 antibodies as well as MAPK pathway inhibitors (MAPKis), targeting BRAF V600 mutant and MEK proteins have significantly improved clinical outcome for patients with CMM. However, multiple clinical trials conducted over the past 5 years indicate that only a subset of patients with CMM have long-term clinical benefit from these therapies (Robert et al., 2019; Topalian et al., 2019).

Loss of DNA mismatch repair causes microsatellite instability, which is associated with response to ICI (Le et al., 2015). *PMS2*, the dimerization partner of MLH1 and integral to mismatch repair, has recently been shown to carry promoter mutations in approximately 10% of melanoma cases, which were associated with more than five-fold higher tumor mutation burden compared with tumors with wild-type *PMS2* (Chalmers et al., 2017).

mutT was first identified in bacteria, and the MutT homolog (MTH1) in humans, encoded by the *NUDT1* gene, is also a DNA repair protein and prevents misincorporation of 8-oxoguanine into DNA. It is often overexpressed in various types of cancer, including CMM (Wang et al., 2018). We recently reported that combining the MTH1 inhibitor TH1579 with a BRAF inhibitor further augments cell death in *BRAFV600* mutant CMM cells compared with either inhibitor alone (Das et al., 2020).

To investigate if the preclinical link between MTH1 and mismatch repair is also clinically relevant, we determined the significance of MTH1 and PMS2 for clinical outcome. We investigated the association of their expression with disease stage and treatment response for ICI and MAPKi using clinical samples from CMM tumors (stages I–IV). This study has been approved by the Regional Ethics Committee in Stockholm, Sweden and has been conducted in accordance with the ethical principles given in the Helsinki Declaration. Written informed consent was obtained from all patients.

The *PMS2* and *MTH1/NUDT1* genes are closely localized on chromosome 7 (7p22.1 and 7p22.3, respectively). The Cancer Genome Atlas analysis highlighted that when sample sets were parsed into *PMS2* and *MTH1* amplifications and deletions, they significantly co-occurred ($P < 0.05$) (Figure 1a). Alterations were significantly associated with shorter disease-free survival ($P = 0.03$) and overall survival ($P = 0.001$) (Supplementary Figure S1). Gain of chromosome 7 has been shown to be a more frequent event in metastatic CMM cases versus primary tumors and has been associated with worse outcome (Bastian et al., 1998) and resistance to MAPKi (Villanueva et al., 2013). Shorter disease-free survival and overall survival was also observed in the The Cancer Genome Atlas patient cohort with altered *MTH1* and *PMS2* mRNA expression (Figure 1b). Furthermore, a correlation between *PMS2* and *MTH1* mRNA expression in the The Cancer Genome Atlas data ($P < 0.0001$) was observed (Figure 1c). This was confirmed in our CMM stage IV cohort by extracting data from previous ampliSEQ analyses (Azimi et al., 2017; Svedman et al., 2019) ($P = 0.0093$) and by qPCR analyses (Supplementary Table S1) on a separate validation cohort ($P = 0.0028$) (Figure 1d and e).

To investigate the clinical relevance of PMS2 and MTH1, we assessed the protein levels using coimmunofluorescence in 61 stage I–IV CMM tumors and 5 normal skin/cancer-adjacent skin tissue (Supplementary Table S2). Eight samples were not evaluable owing to excessive necrotic areas. Compared with stage III–IV, fewer stage I–II tumors and no normal skin/adjacent tissue had high expression of MTH1 (9/31 [29%], 1/22 [5%], and 0/5 [0%], respectively) (Figure 1f and Supplementary Tables S2 and S3), whereas no difference was observed regarding cytoplasmic staining. MTH1 nuclear expression together with nuclear PMS2 expression was only detected in 17 of 31 (55%) stage III/IV but not in earlier stages (Figure 1f and Supplementary Tables S2 and S3), indicating an increased coexpression in advanced disease.

Pretreatment (PRE) metastatic tumors from a subset of the patients with CMM with advanced disease (n = 14) receiving ICI or MAPKi therapies were stained for both MTH1 and PMS2 (Supplementary Table S2). Of 14 cases having moderate/high MTH1 expression together with PMS2 expression, 5 were associated with a short progression free survival (Figure 1g). Paired core biopsies obtained before treatment

Abbreviations: CMM, cutaneous malignant melanoma; ICI, immune checkpoint inhibitor; MAPKi, MAPK pathway inhibitor; PRE, pretreatment

Accepted manuscript published online XXX; corrected proof published online XXX

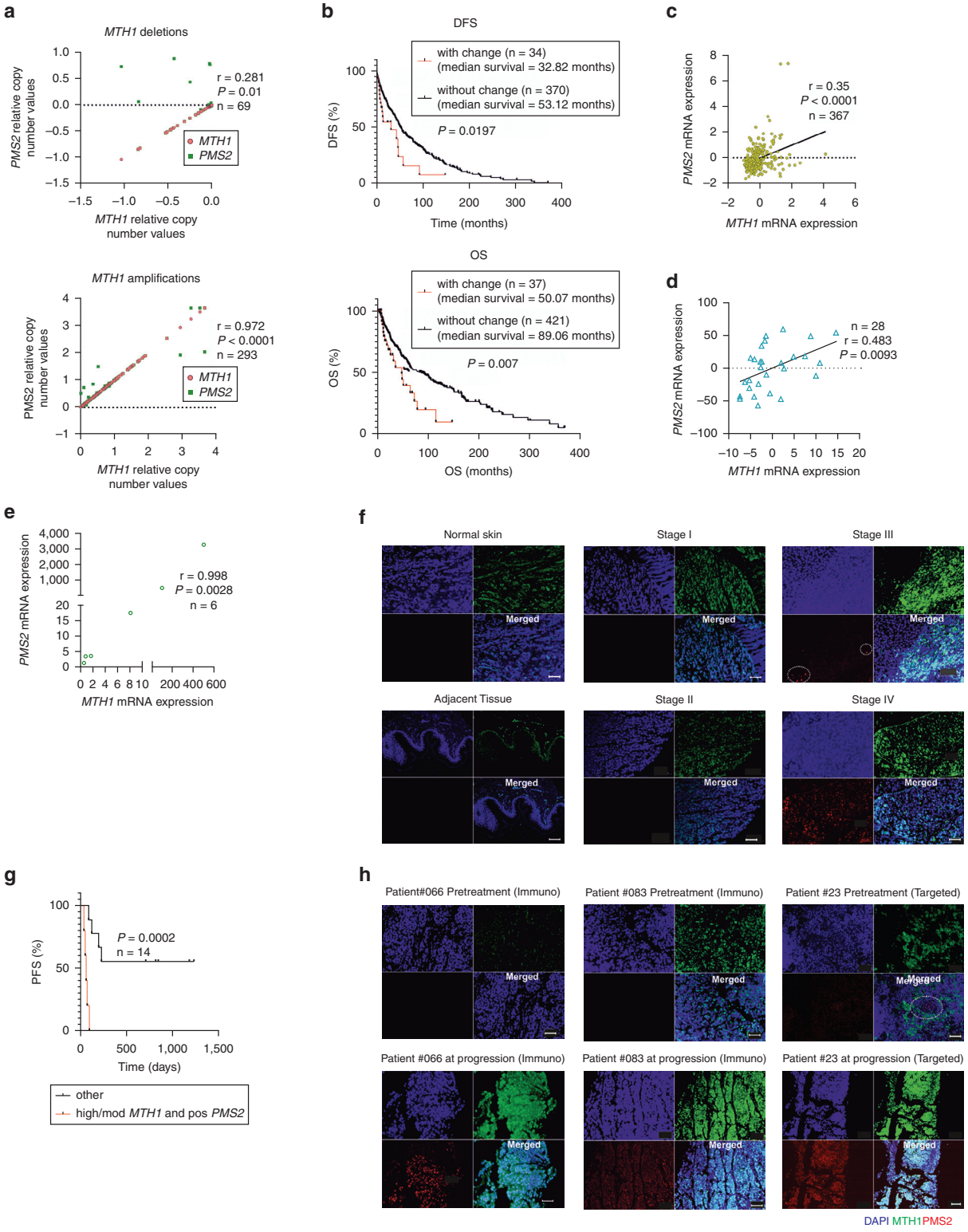

Figure 1. Coexpression at the protein level is observed in advanced stages of CMM and after disease progression to therapy. (**a**) TCGA data show a correlation between *PMS2* and *MTH1* deletions and amplifications. (**b**) Altered *MTH1* and *PMS2* mRNA expression is associated with shorter DFS and OS. (**c**) TCGA mRNA data shows a correlation between *PMS2* and *MTH1*. (**d**) *MTH1* and *PMS2* mRNA correlated in our stage IV cohort and (**e**) in an independent cohort. (**f**) Coexpression of MTH1 (green) and PMS2 (red) proteins is shown in stages III/IV (Bar = 50 μm). (**g**) Survival analysis showing that moderate to high MTH1 expression together with PMS2 expression is associated with shorter PFS. (**h**) Induced protein expression of MTH1 and PMS2 was observed at progression after MAPKi or ICI therapy (Bar = 50 μm). CMM, cutaneous malignant melanoma; DFS, disease-free survival; ICI, immune checkpoint inhibitor; MAPKi, MAPK pathway inhibitor; OS, overall survival; PFS, progression free survival; TCGA, The Cancer Genome Atlas.

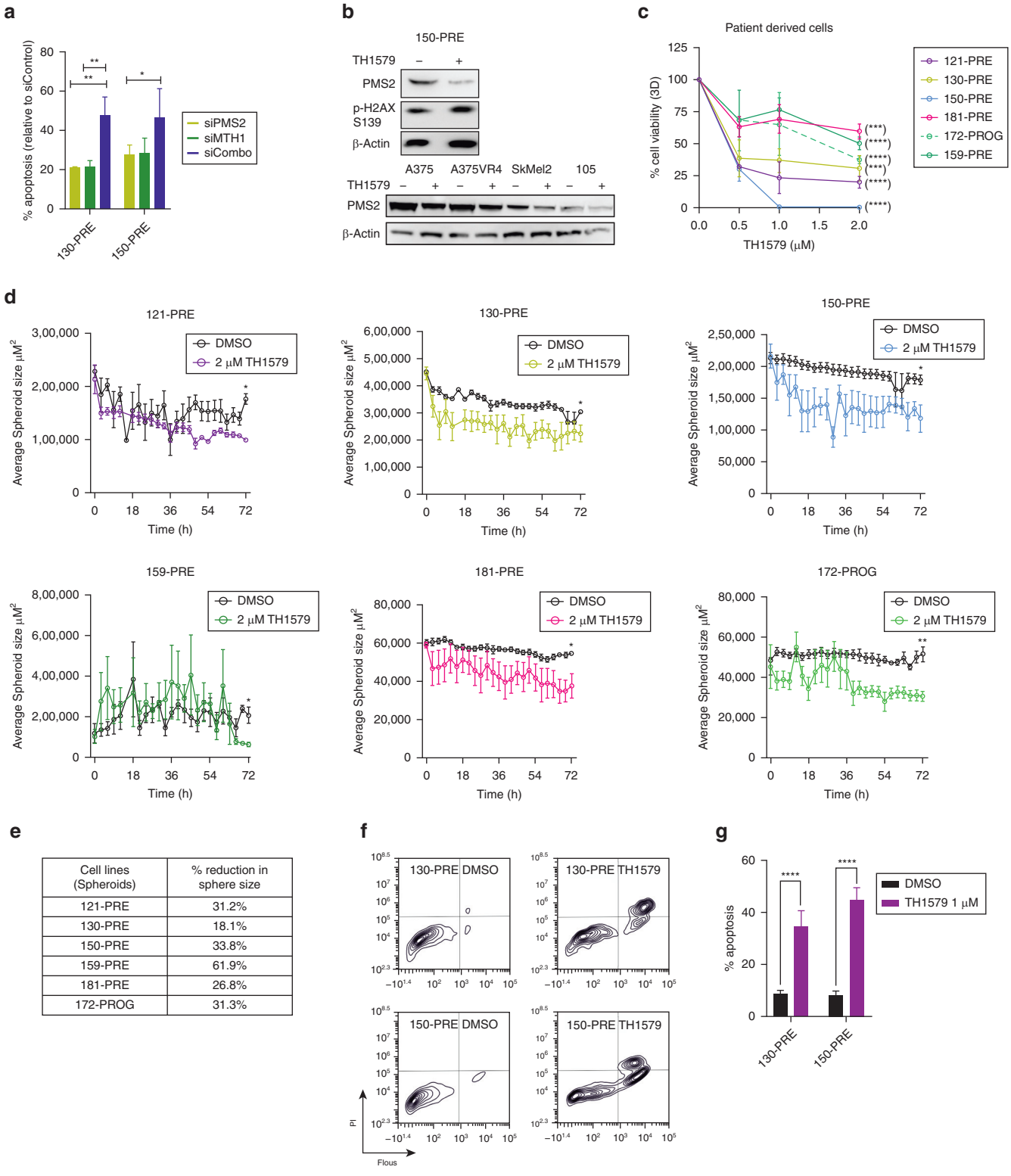

Cell lines (Spheroids)	% reduction in sphere size
121-PRE	31.2%
130-PRE	18.1%
150-PRE	33.8%
159-PRE	61.9%
181-PRE	26.8%
172-PROG	31.3%

Figure 2. TH579 is an effective treatment option for CMM, including ICI-resistant tumor cells. (**a**) Induced apoptosis on cosilencing of *MTH1* and *PMS2* when compared with silencing *MTH1* or *PMS2* alone (Student's *t*-test, n = 3). (**b**) Downregulation of PMS2 and upregulation of p-H2AX in CMM cells after 24-h treatment with 1 μM TH1579 (n = 2). (**c**) Reduced cell viability after 72-h treatment with TH1579 on spheroids generated using patient-derived short-term cell lines (ANOVA test, n = 3) and (**d**) reduction in tumor spheroid sizes (ANOVA test, n = 3). (**e**) % Reduction in sphere area when comparing treatment with DMSO control (Students *t*-test, n = 3). (**f**) Increased apoptosis in patient-derived short-term cell lines after 48-h treatment with 1 μM TH1579. (**g**) Quantification of (**f**) (Student's *t*-test, n = 3). **P* < 0.05, ***P* < 0.01, ****P* < 0.001, *****P* < 0.0001. 3D, three-dimensional; CMM, cutaneous malignant melanoma; h, hour; ICI, immune checkpoint inhibitor; p-H2AX, phosphorylated H2AX; PI, propidium iodide; PRE, pretreatment; PROG, progression; siCombo, Combo small interfering RNA; siControl, control small interfering RNA; siMTH1, *MTH1* small interfering RNA; siPMS2, *PMS2* small interfering RNA.

start and after progression from the same tumor/localization in patients receiving ICI or MAPKi (Supplementary Table S2) demonstrated upregulation of MTH1 and PMS2 expression levels after disease progression in all cases (Figure 1h).

Additionally, we investigated the effects of cosilencing *MTH1* and *PMS2* (Supplementary Table S4) using two patient-derived short-term cell lines (Supplementary Table S5), 130-PRE and 150-PRE, obtained from patients before receiving ICI. Our analysis revealed that an increased induction of apoptosis with cosilencing *MTH1* and *PMS2* (~45−55%), compared with silencing either gene alone (20%), was significant ($P < 0.01$) in 130-PRE but did not reach significance ($P = 0.07$) in 150-PRE (Figure 2a).

We and others have shown that the MTH1 inhibitor TH1579 is a potent drug for a wide range of cancers, including CMM (Einarsdottir et al., 2018). We investigated and found that TH1579 also reduces the expression of PMS2 in CMM cell lines (Figure 2b and Supplementary Figure S2). We further demonstrated that the treatment caused elevated phosphorylated H2AX, a marker of DNA damage, in 150-PRE (Figure 2b and Supplementary Figure S2). To confirm the potency of TH1579 in a panel of patient-derived short-term cells sensitive or resistant to ICI (Supplementary Table S5), a spheroid model was employed, in which cells were treated with TH1579 for 72 hours. All cell lines showed reduced viability (40−99%) (Figure 2c) and reduction of tumor spheroid area by TH1579, including a cell line (172-progression) established from a patient who progressed on ICI ($P < 0.05$) (Figure 2d and e). We validated and found that a reduction in cell viability after TH1579 treatment is due to a significant induction of cell death in 130-PRE and 150-PRE (~35−55%, $P < 0.0001$) (Figure 2f and g).

Herein, we propose that TH1579 could be a good complement to ICI or MAPKi therapy, particularly in non-responding patient cohorts. TH1579 also downregulated PMS2 and induced cytotoxicity in both ICI-sensitive and -resistant CMM patient-derived short-term cultures. Our experimental evidence highlights that treatment of CMM cells with TH1579 or, alternatively, concomitant silencing of *MTH1* and *PMS2* invokes a higher induction of cell death. A limitation of this study is the small sample set; further follow-up studies with larger patient cohorts are therefore warranted to validate this hypothesis and hopefully implement it into clinical practice.

Data availability statement

Datasets related to this article can be found in the Supplementary information hosted at www.jidonline.org.

ORCIDs

Ishani Das: http://orcid.org/0000-0002-2019-8072
Rainer Tuominen: http://orcid.org/0000-0002-5871-3682
Thomas Helleday: http://orcid.org/0000-0002-7384-092X
Johan Hansson: http://orcid.org/0000-0002-2618-3779
Ulrika Warpman Berglund: http://orcid.org/0000-0002-6372-1396
Suzanne Egyházi Brage: http://orcid.org/0000-0002-0524-2346

CONFLICT OF INTEREST

A patent has been filed with TH1579 where TH is listed as inventor. The Intellectual Property Right is owned by the nonprofit Thomas Helleday Foundation for Medical Research where TH and UWB are board members. Thomas Helleday Foundation for Medical Research is a sponsor for an ongoing clinical trial with TH1579. Oxcia AB is assisting Thomas Helleday Foundation for Medical Research in the TH1579 clinical trial. UWB is CEO of Oxcia AB, and UWB and TH are shareholders in Oxcia AB. The remaining authors state no conflict of interest.

ACKNOWLEDGMENTS

Thanks to the oncologists Maria Wolodarski, Hildur Helgadóttir, Giuseppe Masucci, Hanna Eriksson, and Johan Falkenius and the nurse Lena Westerberg in supporting us with the inclusion of patients in this work. We thank Karl-Johan Ekdahl for helping us in collecting tumor samples, Fernanda Costa Svedman for clinical data, Marianne Frostvik Stolt for preparation of the clinical samples, Veronica Höiom for analyzing ampliSEQ data, and National Genomics Infrastructure Uppsala, Genome Center, and UPPMAX for providing assistance in massive parallel sequencing and computational infrastructure. This work is supported by grants from The Cancer Research Funds of Radiumhemmet (174153, JH), the Swedish Cancer Society (CAN 2017-733, JH), Knut and Alice Wallenberg foundation (2013-0093, JH [coapplicant]), Torsten and Ragnar Söderberg Foundation (TH), and Swedish Foundation for Strategic Research (RB13-0224, UWB).

AUTHOR CONTRIBUTIONS

Conceptualization: ID, RT, UWB, SEB; Formal Analysis: ID, RT, SEB; Funding Acquisition: TH, JH, UWB; Investigation: ID, RT; Methodology: ID, RT; Project Administration: TH, JH, UWB, SEB; Resources: JH; Supervision: TH, JH, UWB, SEB; Validation: ID, RT, SEB; Writing - Original Draft Preparation: ID, RT, SEB; Writing - Review and Editing: ID, RT, TH, JH, UWB, SEB

***Ishani Das*[1], *Rainer Tuominen*[1], *Thomas Helleday*[2,3], *Johan Hansson*[1], *Ulrika Warpman Berglund*[2,4] and *Suzanne Egyházi Brage*[1,*]**

[1]*Department of Oncology-Pathology, Karolinska Institutet, Stockholm, Sweden;* [2]*Science for Life Laboratory, Department of Oncology-Pathology, Karolinska Institutet, Stockholm, Sweden;* [3]*Weston Park Cancer Centre, Department of Oncology and Metabolism, The University of Sheffield, Sheffield, United Kingdom; and* [4]*Oxcia AB, Stockholm, Sweden*

[*]*Corresponding author e-mail: suzanne.egyhazi.brage@ki.se*

SUPPLEMENTARY MATERIAL

Supplementary material is linked to the online version of the paper at www.jidonline.org, and at https://doi.org/10.1016/j.jid.2021.07.166.

REFERENCES

Alexandrov LB, Nik-Zainal S, Wedge DC, Aparicio SA, Behjati S, Biankin AV, et al. Signatures of mutational processes in human cancer [published correction appears in Nature 2013;502:258]. Nature 2013;500:415−21.

Azimi A, Tuominen R, Costa Svedman F, Caramuta S, Pernemalm M, Frostvik Stolt M, et al. Silencing FLI or targeting CD13/ANPEP lead to dephosphorylation of EPHA2, a mediator of BRAF inhibitor resistance, and induce growth arrest or apoptosis in melanoma cells. Cell Death Dis 2017;8:e3029.

Bastian BC, LeBoit PE, Hamm H, Bröcker EB, Pinkel D. Chromosomal gains and losses in primary cutaneous melanomas detected by comparative genomic hybridization. Cancer Res 1998;58:2170−5.

Chalmers ZR, Connelly CF, Fabrizio D, Gay L, Ali SM, Ennis R, et al. Analysis of 100,000 human cancer genomes reveals the landscape of tumor mutational burden. Genome Med 2017;9:34.

Das I, Gad H, Bräutigam L, Pudelko L, Tuominen R, Höiom V, et al. AXL and CAV-1 play a role for MTH1 inhibitor TH1579 sensitivity in cutaneous malignant melanoma. Cell Death Differ 2020;27:2081−98.

Einarsdottir BO, Karlsson J, Söderberg EMV, Lindberg MF, Funck-Brentano E, Jespersen H, et al. A patient-derived xenograft pre-clinical trial reveals treatment responses and a resistance mechanism to karonudib in metastatic melanoma [published correction appears in Cell Death Dis 2020;11:99]. Cell Death Dis 2018;9:810.

Le DT, Uram JN, Wang H, Bartlett BR, Kemberling H, Eyring AD, et al. PD-1 blockade in tumors with mismatch-repair deficiency. N Engl J Med 2015;372:2509−20.

Mouw KW, Goldberg MS, Konstantinopoulos PA, D'Andrea AD. DNA damage and repair biomarkers of immunotherapy response. Cancer Discov 2017;7:675−93.

Robert C, Grob JJ, Stroyakovskiy D, Karaszewska B, Hauschild A, Levchenko E, et al. Five-year outcomes with dabrafenib plus

trametinib in metastatic melanoma. N Engl J Med 2019;381:626–36.

Svedman FC, Das I, Tuominen R, Ramqvist ED, Hansson J, Höiom V, et al. Genes involved in DNA replication, chromatin remodeling and cell cycle as potential biomarkers for therapy outcome to immune therapy in patients with metastatic cutaneous malignant melanoma. Ann Oncol 2019;30:v559.

Topalian SL, Hodi FS, Brahmer JR, Gettinger SN, Smith DC, McDermott DF, et al. Five-year survival and correlates among patients with advanced melanoma, renal cell carcinoma, or non-small cell lung cancer treated with nivolumab. JAMA Oncol 2019;5:1411–20.

Villanueva J, Infante JR, Krepler C, Reyes-Uribe P, Samanta M, Chen HY, et al. Concurrent MEK2 mutation and BRAF amplification confer resistance to BRAF and MEK inhibitors in melanoma. Cell Rep 2013;4:1090–9.

Wang L, Leite de Oliveira R, Huijberts S, Bosdriesz E, Pencheva N, Brunen D, et al. An acquired vulnerability of drug-resistant melanoma with therapeutic potential. Cell 2018;173:1413–1425.e14.

SUPPLEMENTARY MATERIALS AND METHODS

Clinical samples

Clinical samples were collected as formalin-fixed, paraffin-embedded from pathology archives at Karolinska University Hospital (Stockholm, Sweden), fresh fine needle aspirates (for establishing short-term cell culture), or core biopsies in cell culture medium or RNAlater from 41 patients with cutaneous malignant melanoma with stage IV disease obtained before start of treatment with MAPK pathway inhibitor (BRAF inhibitor alone or in combination with MEK inhibitor) or immune checkpoint inhibitor or during treatment and/or at progression of disease. An additional 10 stage III/IV formalin-fixed, paraffin-embedded samples (treatment unknown) were also collected (Supplementary Table S2). Tissue microarray was purchased from US Biomax (Rockville, MD) (ME 1002A), including primary cutaneous malignant melanoma tumors (stage I–IV) and normal skin. Data from The Cancer Genome Atlas was used to perform copy number variation, mRNA expression, and survival analyses.

Cell culture

A375VR4, a *BRAF*V600E mutated BRAF inhibitor (vemurafenib)–resistant cell line was derived in-house from A375 ATCC (Manassas, VA) (Azimi et al., 2017). *NRAS* mutant SkMel2 (Q61R) was purchased from ATCC, and the *BRAF/NRAS* wild-type cell line ESTDAB105 was purchased from European Searchable Tumor Line Database and Cell Bank. *BRAF* mutant cell lines were cultured in minimal essential medium, and *NRAS* mutant and *BRAF/NRAS* wild-type cells were cultured in RPMI-1640 according to manufacturer's protocol. All cell lines were confirmed to be mycoplasma free. For all experiments on clinical patient material, short-term derived cell lines patients with cutaneous malignant melanoma (generated in-house originating from fine needle aspirates obtained pre- or posttreatment, see Supplementary Table S5) were cultured in DMEM (Gibco, Waltham, MA) with 10% fetal bovine serum.

Cell viability assay (CellTitre-3D)

Spheres were formed using the hanging drop method as previously described (Das et al., 2019). Spheres were treated with different concentrations of TH1579 (0.5, 1.0, and 2.0 μM) for 72 hours. During this period, live cell imaging was performed every third hour by Incucyte (Sartorius, Göttingen, Germany). Cell viability was measured using CellTiter 3D (Promega, Madison, WI) solution according to manufacturer's protocol followed by measurement of luminescence by Tecan Spark 10M microplate reader (Tecan Trading AG, Männedorf, Switzerland).

Small interfering RNA transfection

Patient-derived cells (130-PRE and 150-PRE) were transfected with small interfering RNA against control, *MTH1*, *PMS2*, or both using Lipofectamine 2000 according to manufacturer's protocol. For sequences of small interfering RNA, see Supplementary Table S4.

Flow cytometry

Annexin V and propidium iodide staining signals (Sigma-Aldrich Chemie Gmbh, Munich, Germany) were measured by flow cytometry (Novocyte 3000, San Diego, CA). A minimum of 7,000 events were measured using polygonal gating to exclude debris and analyzed using Novoexpress software (ACEA Biosciences, San Diego, CA) to determine induction of apoptosis.

Immunoblotting

Protein was isolated using premade RIPA buffer (Santa Cruz Biotechnology, Dallas, TX) and supplemented with additional protease (Santa Cruz Biotechnology) and phosphatase inhibitor cocktails (Sigma-Aldrich Chemie Gmbh). Protein concentration was measured using BCA (Thermo Fisher Scientific, Waltham, MA), and immunoblotting was performed as per manufacturer's guidelines. Membranes were incubated overnight with primary antibodies against MTH1 (1:1,000, Novus Biologicals, Littleton, CO) and PMS2 (1:1,000, Novus Biologicals), followed by secondary antibody incubation with anti-rabbit (1:1,000) or anti-mouse (1:2,000) (Cell Signaling Technology, Danvers, MA). Signal detection was performed using Image Quant LAS 4000 (GE Healthcare Europe GmbH, Freiburg, Germany).

Immunofluorescence

Immunofluorescence was performed on tissue microarray and formalin-fixed, paraffin-embedded samples as previously described on manufacturer's website (Novus Biologicals). Briefly, sections were dehydrated and antigen retrieval was performed using citrate buffer. Sections were stained overnight with anti-MTH1 (1:100, Novus Biologicals) or anti-PMS2 (1:100, BD Biosciences, Allschwil, Switzerland), washed, incubated with secondary antibodies (1:200, rabbit Alexa Fluor 488 or mouse Alexa Fluor 594, Cell Signaling Technology), mounted with DAPI (Sigma-Aldrich), and visualized and imaged using AxioImager M2 (Zeiss, Oberkochen, Germany). The intensity (negative, low, moderate, or high) of MTH1- and PMS2-positive tumor cells was evaluated. Specimens with low expression had the majority of tumor cells with a staining intensity of 1, moderate when the majority of tumor cells had a staining intensity of 2, and high when the majority of tumor cells had a staining intensity of 3.

The Cancer Genome Atlas data sets

The skin cutaneous melanoma dataset from cBioPortal has been used to analyze associations of *MTH1* and *PMS2* to progression free survival and overall survival (Cerami et al., 2012; Gao et al., 2013).

RNA extraction and qPCR

RNA was extracted from clinical samples and qPCR was performed as previously described (Das et al., 2019). Details for primers used in this study can be found in Supplementary Table S1.

Statistical analysis

All experiments were conducted in triplicate, and results were presented as mean ± SD or mean ± SEM as mentioned in figure legends. All statistical analyses were carried out using GraphPad Prism version 7.0 and version 8.0 (GraphPad Software, San Diego, CA). To compare difference and Spearman rank correlation between two groups, Student's *t*-test was employed. To compare differences between multiple groups, one-way ANOVA test was used. For comparing patient survival data, Mantel-Cox log-rank test was employed.

SUPPLEMENTARY REFERENCES

Azimi A, Tuominen R, Costa Svedman F, Caramuta S, Pernemalm M, Frostvik Stolt M, et al. Silencing FLI or targeting CD13/ANPEP lead to dephosphorylation of EPHA2, a mediator of BRAF inhibitor resistance, and induce growth arrest or apoptosis in melanoma cells. Cell Death Dis 2017;8:e3029.

Cerami E, Gao J, Dogrusoz U, Gross BE, Sumer SO, Aksoy BA, et al. The cBio cancer genomics portal: an open platform for exploring multidimensional cancer genomics data [published correction appears in Cancer Discov 2012;2:960]. Cancer Discov 2012;2:401–4.

Das I, Wilhelm M, Höiom V, Franco Marquez R, Costa Svedman F, Hansson J, et al. Combining ERBB family and MET inhibitors is an effective therapeutic strategy in cutaneous malignant melanoma independent of BRAF/NRAS mutation status. Cell Death Dis 2019;10:663.

Gao J, Aksoy BA, Dogrusoz U, Dresdner G, Gross B, Sumer SO, et al. Integrative analysis of complex cancer genomics and clinical profiles using the cBioPortal. Sci Signal 2013;6:pl1.

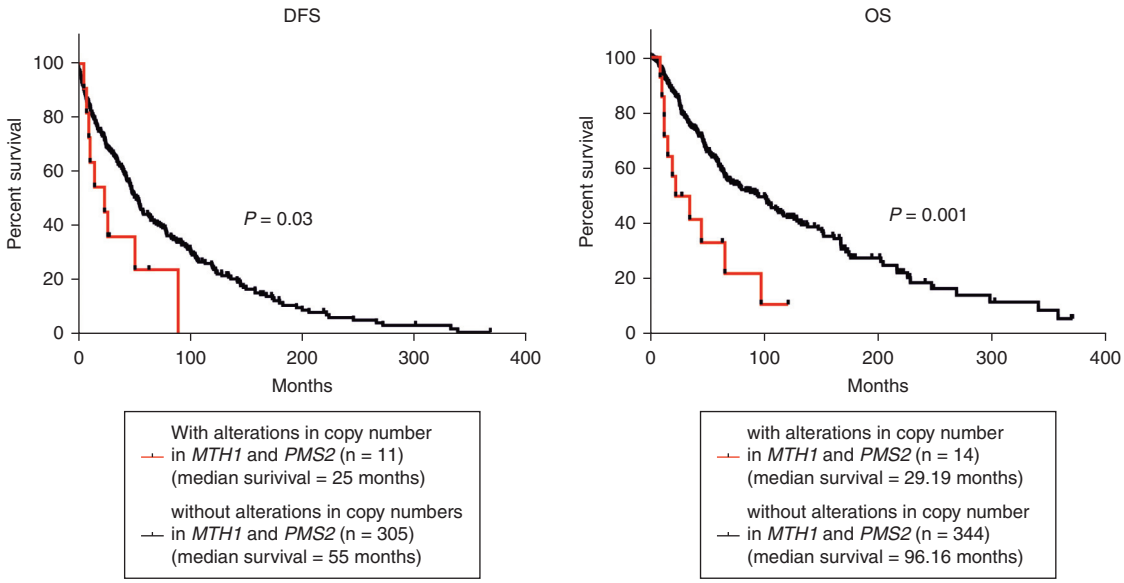

Supplementary Figure S1. Kaplan-Meier curves showing shorter disease-free and overall survival in patients with CMM with CNV alterations in *MTH2* and *PMS2*. CNV in *MTH1* and *PMS2* is associated with shorter disease-free survival (n = 316, $P = 0.03$) and overall survival (n = 358, $P = 0.001$). CMM, cutaneous malignant melanoma; CNV, copy number variation.

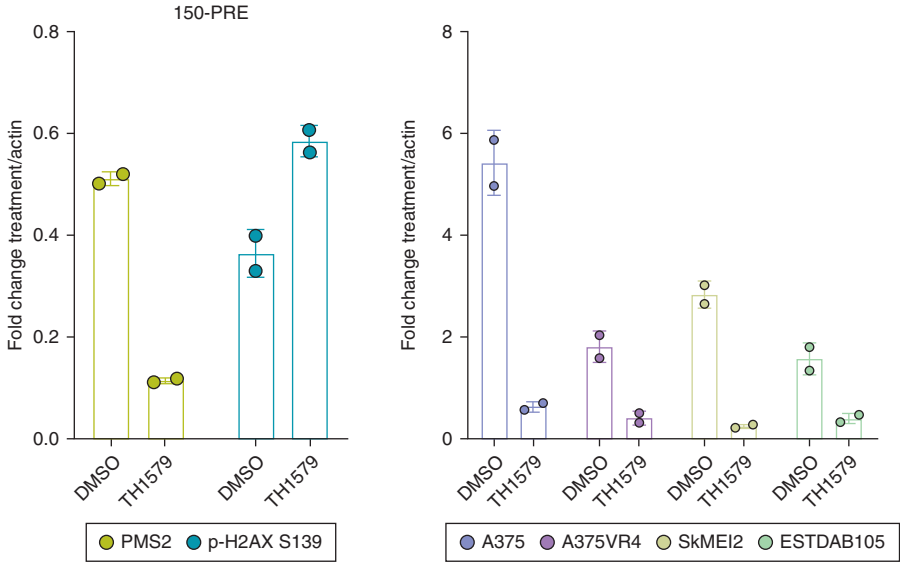

Supplementary Figure S2. TH1579 treatment reduces PMS2 and induces p-H2AX protein levels in CMM cell lines. Quantification of WB (Figure 2b) showing fold change in PMS2 and p-H2AX normalized to actin loading control on treatment with DMSO or 1 μM TH1579 for 24 hours (n = 2). p-H2AX, phosphorylated H2AX; WB, western blot.

Supplementary Table S1. Primers Used for qPCR in this Study

Gene	Gene #	Source	Sequence	PCR Product Length (bp)
MTH1	4521	Merck Sigma-Aldrich	5′-AGTTGGAGTGGGAAGAAC-3′	154
MTH1	4521	Merck Sigma-Aldrich	5′-CTCCTTCTTGCACTTTGC-3′	—
PMS2	5395	Merck Sigma-Aldrich	5′-GGGTAGAAGAAGAAAACTTCG-3′	99
PMS2	5395	Merck Sigma-Aldrich	5′-GAAAGCCAAAAGTTTCAACC-3′	—
HPRT1	3521	Eurofins AG	5′-GACACTGGCAAAACAATGCAGAC-3′	93
HPRT1	3521	Eurofins AG	5′-GGTCCTTTTCACCAGCAAGCT-3′	—
HMBS	3145	Eurofins AG	5′-ACAACCGGGTGGGGCAGA-3′	111
HMBS	3145	Eurofins AG	5′-CCACCAGATCCAAGATGTCCTG-3′	—

Abbreviation: bp, base pair.

Supplementary Table S2. A Summary of the Evaluation of MTH1 and PMS2 Protein Expression in Primary CMM (Stage I–IV) and Normal Skin in TMA (ME 1002a) and Additional 29 Stage III/IV Metastatic Samples Using Immunofluorescence

Position on TMA or Patient No	Stage	Type of Lesion	MTH1 Nuclear Expression	MTH1 Cytoplasmic Expression	PMS2 Nuclear Expression
A1/A2	IIB	Primary	Low	ND	ND
A3/A4	III	Primary	Moderate	Moderate	ND
A5/A6	IIB	Primary	Moderate	Moderate	ND
A7/A8	IIA	Primary	NE	NE	ND
A9/A10	IIB	Primary	Moderate	Moderate	ND
B1/B2	IA	Primary	ND	Low	ND
B3/B4	IIB	Primary	Moderate	Moderate	ND
B5/B6	IIB	Primary	Moderate	Moderate	ND
B7/B8	IIB	Primary	Low	ND	ND
B9/B10	IIB	Primary	Low	Low	ND
C1/C2	III	Primary	Moderate	Few Moderate	ND
C3/C4	IIB	Primary	High	ND	ND
C5/C6	IIB	Primary	Moderate	Moderate	ND
C7/C8	IIB	Primary	Low	ND	ND
C9/C10	IIB	Primary	NE	NE	ND
D1/D2	III	Primary	High	Few High	ND
D3/D4	IB	Primary	Low	Low	ND
D5/D6	IIB	Primary	NE	NE	ND
D7/D8	III	Primary	Moderate	ND	Low
D9/D10	IIB	Primary	ND	Low	ND
E1/E2	IIB	Primary	NE	Ne	ND
E3/E4	IIB	Primary	Low	Low	ND
E5/E6	IIB	Primary	Moderate	Moderate	ND
E7/E8	IIA	Primary	NE	NE	ND
E9/E10	IIB	Primary	NE	NE	ND
F1/F2	IIB	Primary	Low	Low	ND
F3/F4	IIB	Primary	Moderate	Moderate	ND
F5/F6	IV	Primary	High	Few High	Moderate
F7/F8	IB	Primary	Low	Low	ND
F9/F10	III	Primary	Moderate	ND	ND
G1/G2	IIB	Primary	NE	NE	ND
G3/G4	IIB	Primary	Moderate	Moderate	ND
G5/G6	IIB	Primary	Low	Low	ND
G7/G8	IIC	Primary	Moderate	Moderate	ND
G9/G10	IIB	Primary	Moderate	Moderate	ND
J1/J2	Cancer-adjacent skin tissue	Normal	Low	Low	ND

(*continued*)

Supplementary Table S2. Continued

Position on TMA or Patient No	Stage	Type of Lesion	MTH1 Nuclear Expression	MTH1 Cytoplasmic Expression	PMS2 Nuclear Expression
J3/J4	Normal skin	Normal	Low	Low	ND
J5/J6	Normal skin	Normal	Low	Low	ND
J7/J8	Normal skin	Normal	ND	Low	ND
J9/J10	Normal skin	Normal	ND	Low	ND
1	III	Metastatic	ND	Moderate	ND
2	III	Metastatic	NE	NE	NE
3	III	Metastatic	High	ND	ND
4	III	Metastatic	Moderate	Moderate	ND
5	III	Metastatic	High	ND	Low
6	IV	Metastatic	Moderate	ND	Moderate
7	IV	Metastatic	High	High	Low
8	IV	Metastatic	High	High	Low
9	IV	Metastatic	High	ND	Low
10	IV	Metastatic	Moderate	ND	Low

Patient No	Stage Type of Lesion	MTH1 Nuclear Expression	MTH1 Cytoplasmic Expression	PMS2 Nuclear Expression	Therapy	Response	PFS (Days)
019-PRE (excision)	IV Metastatic	Moderate	Moderate	Moderate	V	NR	35
003-PRE (excision)	IV Metastatic	Moderate	ND	Low	V	NR	60
040-PRE (excision)	IV Metastatic	High	moderate	Low	D + T	NR	70
026-PRE (excision)	IV Metastatic	High	Low	Moderate	V	NR	95
023-PRE:1 (excision)	IV Metastatic	Low	Low	ND	V	DC	224
023-PRE:2 (core)	IV Metastatic	Low	Moderate	Low	V	DC	224
023-PROG:2 (core)	IV Metastatic	High	Low	Moderate	V	DC	224
112-PRE (excision)	IV Metastatic	Low	Low	Low	P	DC	847[1]
065-PRE (excision)	IV Metastatic	Moderate	Moderate	ND	N	DC	1,183[1]
127-PRE	IV Metastatic	ND	Low	ND	N	DC	708[1]
113-PRE	IV Metastatic	Low	ND	Few low	P	DC	820[1]
109-PRE	IV Metastatic	Moderate	Moderate	High	P + E	NR	49
058-PRE (excision)	IV Metastatic	Low	Moderate	Low	N	DC	196
058-PRE (core)	IV Metastatic	ND	Low	ND	N	DC	196
059-PRE (excision)	IV Metastatic	Few low	Few low	ND	N	DC	1,228[1]
066-PRE (core)	IV Metastatic	Moderate	Low	ND	N	NR	119
066-PROG (core)	IV Metastatic	Moderate	Low	High	N	NR	119
083-PRE (core)	IV Metastatic	ND	Low	ND	N	NR	91
083-PROG (core)	IV Metastatic	Moderate	Low	Low	N	NR	91

Abbreviations: CMM, cutaneous malignant melanoma; D, dabrafenib; E, epacadostat; N, nivolumab; ND, not detectable; NE, not evaluable; No, number; P, pembrolizumab; PFS, progression free survival; PRE, pretreatment; PROG, progression; T, trametinib; TMA, tissue microarray; v, vemurafenib.
[1]Patients still responding to treatment.

Supplementary Table S3. Table Summarizing the Evaluation of MTH1 and PMS2 Staining Using Immunofluorescence

Sample	MTH1 Nuclear Expression	MTH1 Cytoplasmic Expression	PMS2 Nuclear Expression
Normal skin (n = 4)	ND (n = 2) Low (n = 2)	Low (n = 4)	ND (n = 4)
Cancer-adjacent skin tissue (n = 1)	Low (n = 1)	Low (n = 1)	ND (n = 1)
Stage I (n = 3)	ND (n = 1) Low (n = 2)	Low (n = 3)	ND (n = 3)
Stage II (n = 19)	ND (n = 1) Low (n = 7) Moderate (n = 10) High (n = 1)	ND (n = 4) Low (n = 5) Moderate (n = 10)	ND (n = 19)
Stage III (n = 9) Primary (n = 5) Metastatic (n = 4)	Moderate (n = 4) High (n = 1) ND (n = 1) Moderate (n = 1) High (n = 2)	ND (n = 2) Moderate (n = 2) High (n = 1) ND (n = 2) Moderate (n = 2)	ND (n = 4) Low (n = 1) ND (n = 3) Low (n = 1)
Stage IV (n = 22) Primary (n = 1) Metastatic[1] (n = 21)	High ND (n = 3) Low (n = 6) Moderate (n = 7) High (n = 5)	High ND (n = 5) Low (n = 8) Moderate (n = 6) High (n = 2)	Moderate ND (n = 7) Low (n = 10) Moderate (n = 3) High (n = 1)

Abbreviation: ND, not detectable.

[1]Two pretreatment metastases from patient 023 and 058 were analyzed and the tumor with highest expression was included in Supplementary Table S2. Both tumors showed ND or low expression of MTH1 and PMS2.

Supplementary Table S4. siRNA Sequences Used in this Study against *MTH1* and *PMS2*

Sequence #	Supplier	Target Sequence
MTH1 #1	Dharmacon	5′-GACGACAGCUACUGGUUUC-3′
MTH1 #3	Dharmacon	5′-CGACGACAGCUACUGGUUU-3′
PMS2 #1	Dharmacon	5′-UAAUGAAGCUGUUCUGAUA-3′
PMS2 #2	Dharmacon	5′-UCUAUGAGUUCUUUAGCUA-3′

Supplementary Table S5. A Summary of Which Treatments Were Received by the Patients from Whom FNA Samples Were Procured for Establishing Primary Cell Cultures and Clinical Outcome

Cell Lines (Spheroids)	FNA Taken Before/during/after Treatment	Treatment	Response
121-PRE	Before	Pembrolizumab	DC
130-PRE	Before	Nivolumab	DC
150-PRE	Before	Nivolumab + Ipilimumab	DC
159-PRE	Before	Pembrolizumab	DC
181-PRE	During	Nivolumab	DC
172-PROG	After	Nivolumab	NR

Abbreviations: DC, disease control; FNA, fine needle aspirate; NR, nonresponder; PRE, pretreatment; PROG, progression.